Integrative and Comparative Biology

Integrative and Comparative Biology, volume 64, number 2, pp. 611–618
https://doi.org/10.1093/icb/icae076

Society for Integrative and Comparative Biology

SYMPOSIUM

Biomechanics of Insect Flight Stability and Perturbation Response

Tyson L. Hedrick [*,1], Emily Blandford[†] and Haithem E. Taha[‡]

[*]Department of Biology, University of North Carolina at Chapel Hill, 10 South Road, Chapel Hill, NC 27599-3280, USA; [†]Department of Biomedical Engineering, Duke University, 101 Science Drive, Durham, NC 27705, USA; [‡]Department of Mechanical and Aerospace Engineering, Samueli School of Engineering, University of California, Irvine, Irvine, CA 92967, USA

From the symposium "Evolution, Physiology, and Biomechanics of Insect Flight" presented at the annual meeting of the Society for Integrative and Comparative Biology, January 2–6, 2024.

[1]E-mail: thedrick@bio.unc.edu

Synopsis Insects must fly in highly variable natural environments filled with gusts, vortices, and other transient aerodynamic phenomena that challenge flight stability. Furthermore, the aerodynamic forces that support insect flight are produced from rapidly oscillating wings of time-varying orientation and configuration. The instantaneous flight forces produced by these wings are large relative to the average forces supporting body weight. The magnitude of these forces and their time-varying direction add another challenge to flight stability, because even proportionally small asymmetries in timing or magnitude between the left and right wings may be sufficient to produce large changes in body orientation. However, these same large-magnitude oscillating forces also offer an opportunity for unexpected flight stability through nonlinear interactions between body orientation, body oscillation in response to time-varying inertial and aerodynamic forces, and the oscillating wings themselves. Understanding the emergent stability properties of flying insects is a crucial step toward understanding the requirements for evolution of flapping flight and decoding the role of sensory feedback in flight control. Here, we provide a brief review of insect flight stability, with some emphasis on stability effects brought about by oscillating wings, and present some preliminary experimental data probing some aspects of flight stability in free-flying insects.

Introduction

Insects successfully navigate an aerial environment filled with potentially destabilizing perturbations; due to their small body size, disturbances easily rejected by larger flyers might be challenging for insects. Furthermore, as investigation into the unsteady aerodynamics that keep insects aloft revealed the magnitude of the forces produced (Ellington et al. 1996; Dickinson et al. 1999), it also became apparent that even small asymmetries in these forces would be sufficient to produce large changes in orientation, potentially making insects highly maneuverable but adding to the stability challenge. Insects are also equipped with distributed, multifaceted sensory systems that help keep them upright in the air, with an array of rapid sensory responses that help enforce flight stability (Taylor and Krapp 2007; Dahake et al. 2018). However, the rapidly oscillating aerodynamic forces that keep insects aloft also add a rich set of conditions for nonlinear interactions between body motion and wing motion that may stabilize or further destabilize insect flight under different conditions (Hedrick et al. 2009; Taha et al. 2020). Understanding the consequences of these oscillating forces is key to understanding how insects coped with the challenges of flight early in its evolution, as well as fully decoding the neuromechanical mechanisms that underlie extant insect flight stability and maneuverability.

Classical analyses of insect flight stability make an early, underlying assumption that the time-varying flight forces produced throughout the course of a wingbeat cycle can be replaced in a flight dynamics model by their whole-cycle average (e.g., Sun et al. 2007). This intuitive simplification allows direct application of flight dynamics models from fixed and rotatory-winged

Advance Access publication June 19, 2024

aircraft (e.g., Stengel 2005). Analyses beginning with these assumptions commonly end with a matrix of partial derivatives that summarize the effects of a disturbance from a trimmed condition described by a set of state variables, typically encompassing current velocity and orientation in two dimensions (3DOF), for example, Equation (1), or three motion directions and three orientations (6DOF). In Equation (1), longitudinal stability is described by responses to forward velocity, vertical velocity, pitch orientation, and pitch rate all linearized about the trimmed condition representing the actual steady-state values for each of the degrees of freedom in the analysis.

$$\begin{pmatrix} \dot{\overline{u}} \\ \dot{\overline{w}} \\ \dot{\overline{q}} \\ \dot{\overline{\theta}} \end{pmatrix} = \begin{bmatrix} \frac{\overline{X}_u}{m} & \frac{\overline{X}_w}{m} & \frac{\overline{X}_q}{m} & -g \\ \frac{\overline{Z}_u}{m} & \frac{\overline{Z}_w}{m} & \frac{\overline{Z}_w}{q} & 0 \\ \frac{\overline{M}_u}{I_{yy}} & \frac{\overline{M}_w}{I_{yy}} & \frac{\overline{M}_q}{I_{yy}} & 0 \\ 0 & 0 & 1 & 0 \end{bmatrix} \begin{pmatrix} \overline{u} \\ \overline{w} \\ \overline{q} \\ \overline{\theta} \end{pmatrix}. \quad (1)$$

Here, the terms in the matrix, that is, X_u, Z_w, etc., are stability derivatives such that X_u represents the partial derivative of forward force X with respect to forward speed u and so forth. Z is vertical force, w is vertical speed, q is pitch rate, θ is pitch orientation, g is gravity, m is mass, and I_{yy} is pitch moment of inertia. Overbars indicate cycle-averaged quantities and dots indicate rates.

Note that this analysis reveals a lack of "pitch stiffness," or any direct coupling between pitch rate and pitch orientation as shown by the zero, the third row, fourth column of the matrix in Equation (1). This means that there is no factor that directly acts to return a perturbed insect to its original pitch orientation. Thus, when the stability characteristics of insects are examined by populating Equation (1) with values from experiments (e.g., Taylor and Thomas 2003) or simulation (e.g., Sun et al. 2007) and performing an eigenvalue analysis, the common result includes an unstable oscillatory mode. As described by Ristroph et al. (2013) and shown in Fig. 1, this mode arises from the interaction between pitch orientation, horizontal acceleration brought about by a change in pitch altering the direction of the aerodynamic force vector, and the subsequent horizontal velocity driving an increase in aerodynamic drag that causes a pitch-up rotation that overshoots the original condition due to inertia (Fig. 1 C and D). Similar analyses considering alternative 3DOF sets focused on yaw or roll orientation also show similar characteristics, with no restoring torque bringing the animal back to a specific yaw or roll angle. However, responses in these modes are somewhat damped by the extended wings, and (at least in hover) the immediate consequences of a change in roll or yaw orientation are less than that in pitch, so longitudinal stability has received the greatest share of experimental and theoretical attention.

As the above description and depiction (Fig. 1) of longitudinal instability suggests, it arises from the fixed attachment of the direction of aerodynamic force such that changes to body orientation necessarily change force orientation, and the force vector position with respect to the center of mass is constant. Effects that disrupt this linkage offer a road back toward flight stability, as shown in Fig. 1E and F. For example, a computational fluid simulation of the hawkmoth *Manduca sexta* in hovering flight with a fictive stroke plane torque motor that adjusts the wing stroke plane such that the net aerodynamic force vector points upward regardless of body orientation both theoretically and practically restores pitch stability (Zhang et al. 2019). Real *M. sexta*, of course, lack a stroke plane torque motor but are known to alter the orientation of the abdomen with respect to the thorax, an action that both alters the center-of-mass location with respect to the force vector and simultaneously alters the orientation of thorax and its attached wings in the inertial reference frame. Such movements can also effectively stabilize longitudinal motion in hovering flight (Dyhr et al. 2013). Both these routes back to stability require an active response on the part of the insect, and are not underlying properties of flight with flapping wings.

However, consideration of the effect of flapping wings on insect flight stability has also shown that these factors can stabilize different body rotations without necessarily involving an active response on the part of the animal. For example, for an animal in hovering flight with flapping wings moving in the horizontal plane, yaw rotations (i.e., rotation about the vertical axis) speed up the wings on one side of the body while slowing down wings on the other side through each half-stroke (Fig. 2). These enhanced velocities create a substantial damping torque, termed flapping counter-torque (FCT), that rapidly slows yaw rotations (Hedrick et al. 2009). Extending this analysis to a more complex stroke plane and six degrees of freedom of motion reveals that FCT and its linear motion counterpart flapping counter-force contribute to a rapid decay of imposed rotations and movements in lateral and longitudinal motion, but that even with these extra flapping wing effects included, unstable modes remain (Cheng and Deng 2011).

In addition to contributing to stability, FCT and similar effects show how time-varying forces from flapping wings can enhance flight maneuverability, a result developed for animal movement in general by Sefati et al. (2013). The FCT effects exist in large part because of the aerodynamic inefficiency of flying insects. Because their flapping wings act at high angles of attack, both

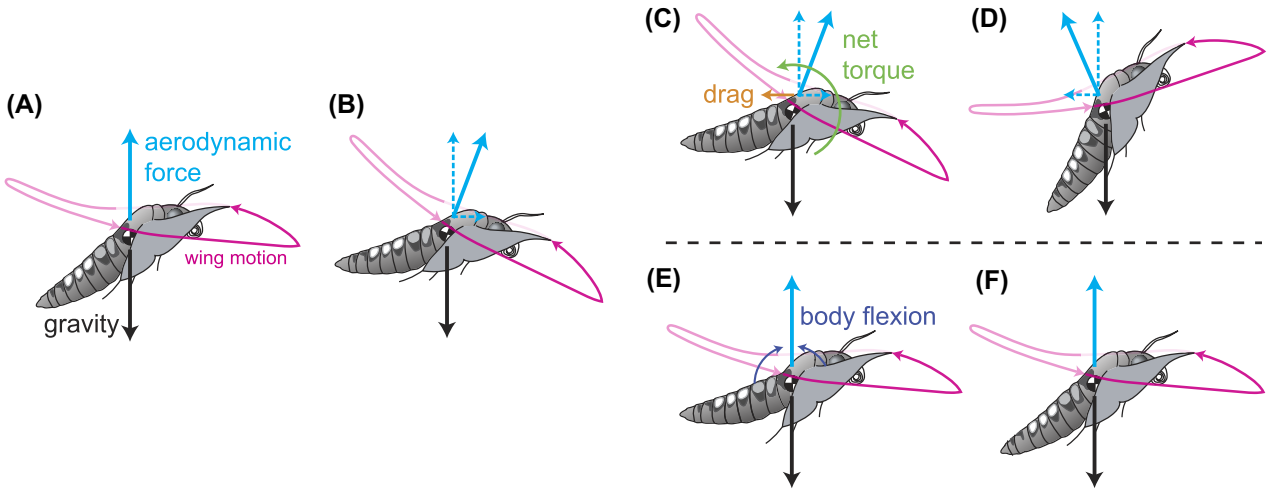

Fig. 1 Two possible outcomes from a hovering insect (A) experiencing a pitch-down perturbation (B) that realigns the aerodynamic force from the wings to produce a forward component. This forward component accelerates the moth, leading to a drag that in combination with gravity will pitch the insect backward as shown in panel (C). For insects with large enough rotational inertia, this pitch overshoots (D) and leads to growing oscillations. However, if the insect restores its stroke plane and aerodynamic force vector to their original orientation by body flexion (or other means) as shown in panel (E), this short-circuits the oscillatory process and allows recovery of the original orientation (F).

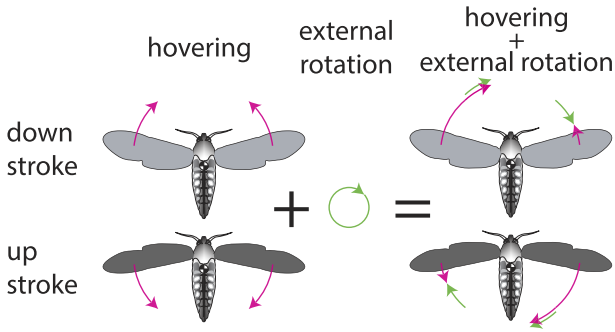

Fig. 2 Simplified depiction of the FCT effect. During unperturbed hovering flight (left side), the wings have symmetric motion with respect to the surrounding air. Addition of an external rotation (right side) differentially enhances the speed of one wing during downstroke, and that of the opposite wing during upstroke. Because aerodynamic torques are proportional to the square of speed and are in a direction opposite to the direction of motion, these torques act against the rotation.

vertical and horizontal forces are large and contribute to the energy cost of flapping in hovering flight. However, the horizontal forces average to zero over a complete cycle, so do not contribute to supporting the animal in the air, but do provide the physical basis for FCT and thus enhance stability. They also contribute to making flying animals maneuverable, because small deviations from symmetry (e.g., a larger flapping amplitude by the left-side wings) produce a net force or torque that pushes the animal into a new orientation, that is, a maneuver. Coupled with the damping effects of FCT once the animal is in motion, such an asymmetry can simplify control of maneuvers because a given degree of asymmetry produces a given maneuvering velocity (rather than acceleration) (Dickson et al. 2010). The larger the underlying opposing forces, the greater the FCT effect, but also the greater the potential for maneuvers. Thus, decreasing flight efficiency offers a route to simultaneously increasing aspects of stability and maneuverability.

As the above paragraphs describe, consideration of the within-wingbeat forces generated by flapping wings revealed some additional damping factors that could contribute to stability, along with a general principle for how animals and machines could sidestep the dictum that stability and maneuverability are opposites, and improving one comes at a cost of the other. However, FCT and similar factors do not provide full dynamical stability for flying insects. As Cheng and Deng (2011) show, unstable modes broadly similar to those identified in the simple, cycle-average force analysis remain, and the presence of even a single unstable mode renders the system as a whole unstable. As described by Taha et al. (2020), a further series of interactions between the within-wingbeat oscillations in body position, pitch orientation, and forward–backward acceleration lead to a vibrational stabilization effect that adds a limited degree of pitch stiffness in longitudinal motion to the model expressed in Equation (1). This effect is nearly sufficient to stabilize longitudinal motion in *M. sexta* where it was first described, but likely less important for smaller insects. This vibrational stabilization mode depends on the forward–backward oscillation in body position with wing flapping, so it is not expected to exist in roll and yaw since symmetric wing motion does not produce oscillations in lateral body position.

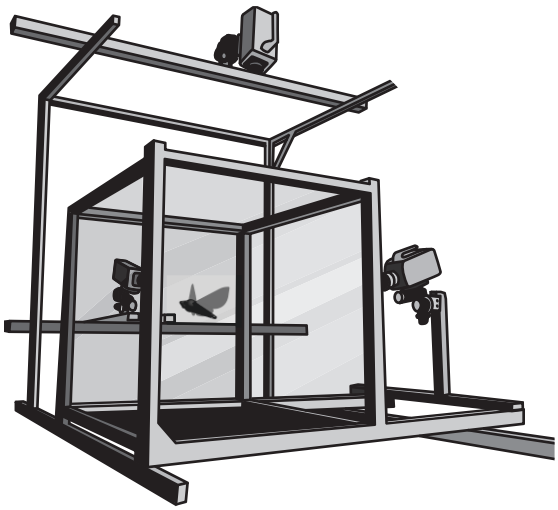

Fig. 3 The moth recording chamber, a glass-walled 0.7 × 0.7 × 0.7 m box with internal infrared illumination (not shown) and high-speed cameras capturing images through mutually orthogonal chamber faces. Figure adapted from Greeter and Hedrick (2016).

Despite the progress made in understanding different aspects of insect flight stability, one remaining challenge is attempting to validate or support these results through animal experiments. The second portion of this manuscript describes preliminary results from two different experiments probing free-flight stability in response to different challenges.

Preliminary experimental results

Here, we describe results from two sets of experiments, both performed on adult male *M. sexta* hawkmoths sourced from the domesticated colony maintained in the Department of Biology, University of North Carolina at Chapel Hill. In both types of experiments, the moths flew in a 0.7 × 0.7 × 0.7 m glass-walled flight chamber equipped with near-infrared (680 nm wavelength) lighting invisible to the hawkmoths (Fig. 3). Three high-speed video cameras, namely Phantom v5.1, Phantom v7.2 (Vision Research Inc., Wayne, NJ), and IDT MotionPro Y4 (Integrated Design Tools Inc., Pasadena, CA) , positioned to approximate nearly orthogonal viewing angles were used to record moth flights and enable three-dimensional kinematic reconstruction of animal motion (Fig. 3). Moths were trained to approach and feed from an artificial flower positioned in the flight chamber. Experiments were conducted with low but not zero visible spectrum lighting from room fluorescent tube lights, typically about 180 lux as measured in the filming chamber with a lux meter (840006, Sper Scientific Ltd). In the first set of experiments, moths approaching the flower were perturbed in flight by a spring-launched projectile that struck them from below and produced pitch-up or pitch-down perturbations, depending on the location where the projectile struck the moth. Results from similar experiments were presented in Taha et al. (2020); some further data are presented here.

In a second set of experiments, moths were trained to fly as described above. Once a control recording showing stable hovering flight was collected, the left and right antenna flagella were trimmed near the base, leaving only 2–4 mm length. As reported by Sane et al. (2007) following such treatment the moths were widely unwilling and/or incapable of sustained flight. However, other sphingid moths such as *Macroglossum stellatarum* will fly after antenna removal (Dahake et al. 2018), and we found that after a 24 h waiting period the *M. sexta* used in our experiments were again willing to fly and feed from the artificial flower, and recordings were made of simple hovering flight during subsequent days.

Following published methodologies in Hedrick (2008) and Theriault et al. (2014), three-dimensional reconstruction of body moth and flight kinematic analysis was conducted using a wand-based camera calibration workflow along with semiautomated but manually supervised tracking of natural landmarks at the abdomen tip, abdomen–thorax junction, and thorax–head junction to continuously measure three-dimensional body orientation, along with wing-tip position at stroke reversals to quantify flapping cycles. Basic aerodynamic expectations for body orientation following perturbation were developed from a blade-element flapping wing simulation tuned to match the performance of a Navier–Stokes numerical simulation of hawkmoth flight (Zheng et al. 2013).

Pitch perturbation

As described previously (Greeter 2017; Taha et al. 2020), the projectile perturbation recordings produce rapid pitch rotational velocities on the order of ±2000 deg/s, with peak rotation rate reached shortly after the projectile collision, but not always coincident with it depending on how the perturbation interacts with the normal flapping-cycle variation in pitch orientation and velocity. Pitch velocity was substantially reduced during the first flapping cycle following the perturbation event, typically decreasing by more than 50% from the maximum recorded magnitude. For example, Fig. 4 shows example pitch perturbation results for a moth, which reaches a maximum downward pitch velocity of 2344 deg/s about 6 ms after the perturbation and during the downstroke phase of the flapping cycle. By the start of the next downstroke, pitch velocity has been reduced to 369 deg/s, or 16% of its peak value. Considering a larger selection of results, a full wingbeat cycle fol-

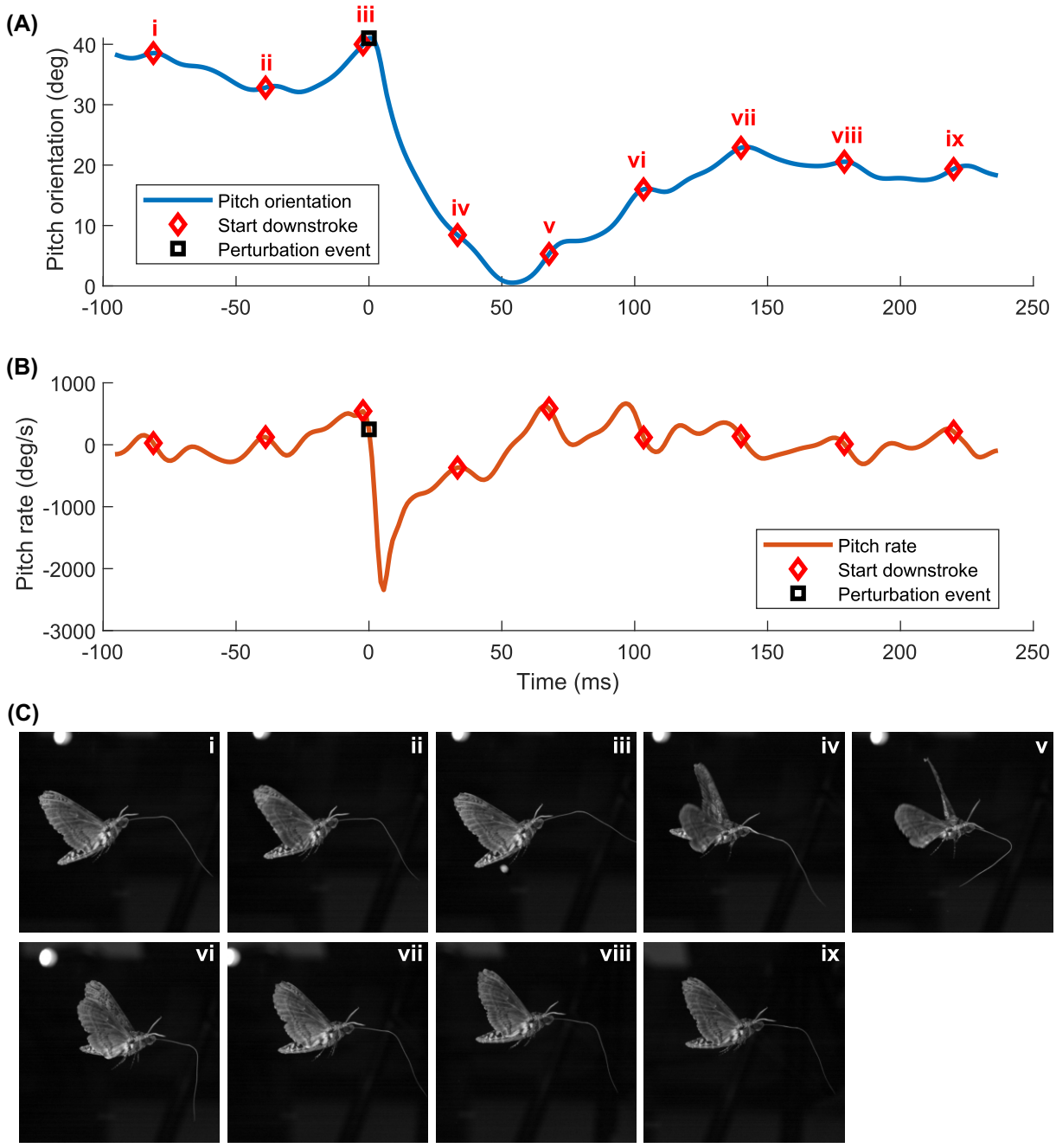

Fig. 4 Results of a pitch perturbation recording from a freely hovering *M. sexta* hawkmoth. Panel (A) shows pitch orientation, panel (B) shows pitch rate, and panel (C) shows a series of still images captured at the start of downstroke of each flapping cycle in the recording. The incoming projectile can be seen in panel (C[iii]) just below the tip of the moth's abdomen. The white circle along the upper edge is a reflection from the infrared lights used to illuminate the scene. Finally, the still images in (C) were cropped from a larger image to keep the moth centered and therefore obscure the small amount of forward motion it undergoes during the perturbation event.

lowing peak perturbation magnitude reduces the original pitch velocity to 16 ± 3% (mean ± std, n=5) of its original value in the first flapping cycle following peak post-perturbation pitch velocity. In comparison, simulations run with a tuned blade-element model of hawkmoth flapping wing aerodynamics (Zheng et al. 2013) across a starting perturbation velocity range from –3000 to 3000 deg/s show a reduction to 61% of the original pitch velocity after a single flapping cycle when averaged across all possible perturbation event times in the flapping cycle. This numerical flapping wing simulation includes FCT effects and body drag, but forces a steady rotation rate and so does not include any physical effects related to acceleration from the perturbation itself or acceleration and deceleration within a flapping cycle. In general, this comparison shows that it would take the

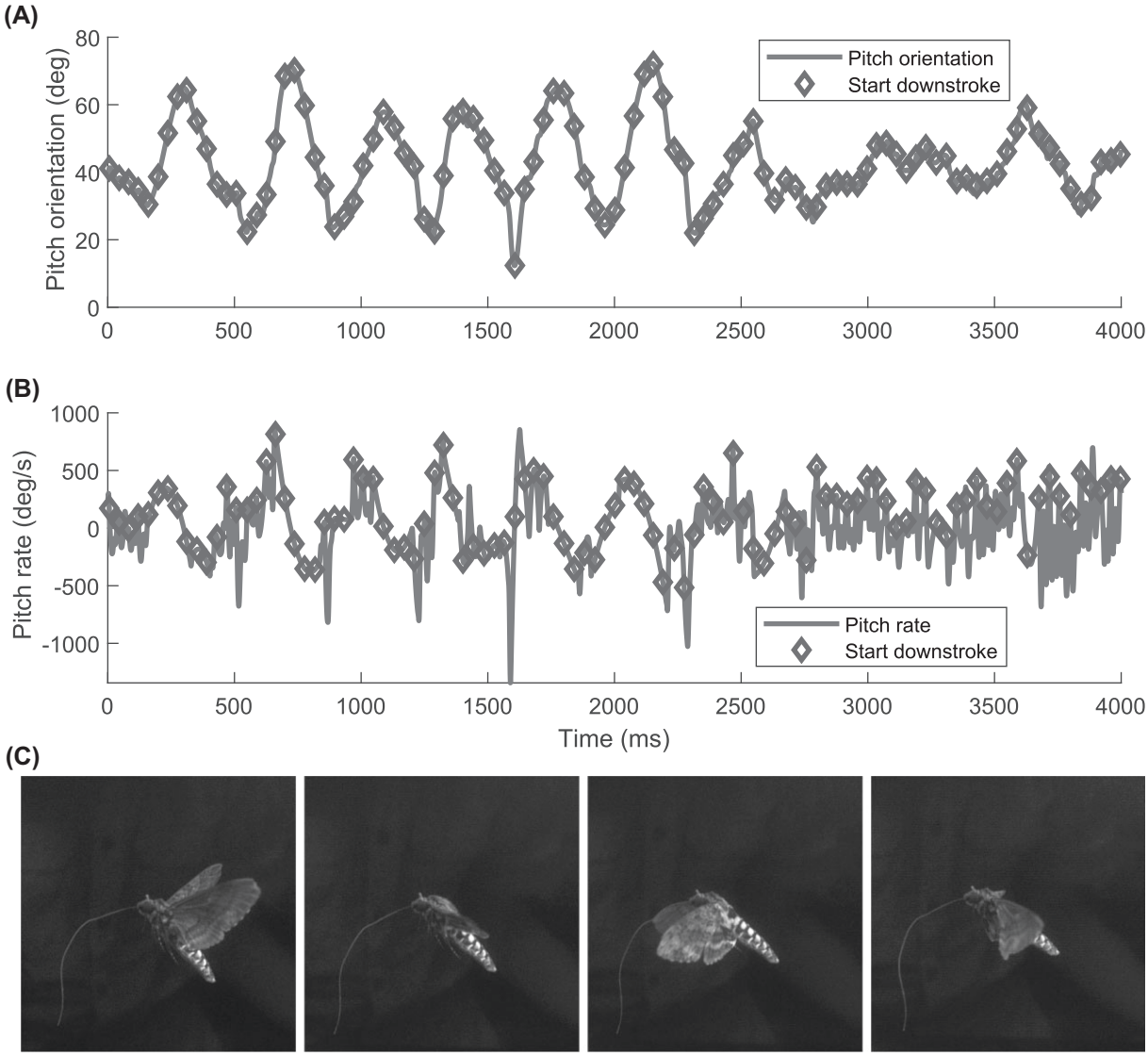

Fig. 5 Four seconds of hovering flight pitch orientation data from an antennectomized moth. Panel (A) shows pitch orientation, panel (B) shows pitch rate, and panel (C) shows a series of still images showing a flapping cycle from start of downstroke to mid-downstroke, start of upstroke, and finally end of upstroke. The long timescale and large amplitude of the slow pitch oscillations shown in panel (A) make it difficult to see the within-cycle pitch oscillations, but these exist and are of similar amplitude to those from moths with intact antennae. The slow, large-amplitude pitch oscillations are not characteristic of typical moth flight, but are also not seen in all instances of antennectomized flight.

simulated moth approximately three flapping cycles to achieve the reduction in perturbation velocity achieved by the actual moth in one cycle.

Antennectomized flight

As described elsewhere, antennectomized hawkmoths are reluctant to fly and perform badly in the air if they do attempt to take flight, with a common although not universal failure mode in the flight chamber of pitching upward and accelerating backward until striking the flight chamber wall. Flight control failures in roll or pitch were unusual in our observation. Previous work demonstrated that using glue to reattach the portion of the flagella clipped off during antennectomy restored most aspects of flight performance (Sane et al. 2007; Dahake et al. 2018). This experiment was not attempted here, and instead we allowed the moths to recover for 24 h after antennectomy, after which they were once again willing and able to fly and hover-feed from the artificial flower. Figure 5 shows the pitch orientation through time of a moth following antennectomy and 24-h recovery. In this instance, a variety of near failures are in evidence, where the moth begins to rapidly pitch upward but then ceases and pitches downward again. However, such dynamics were not

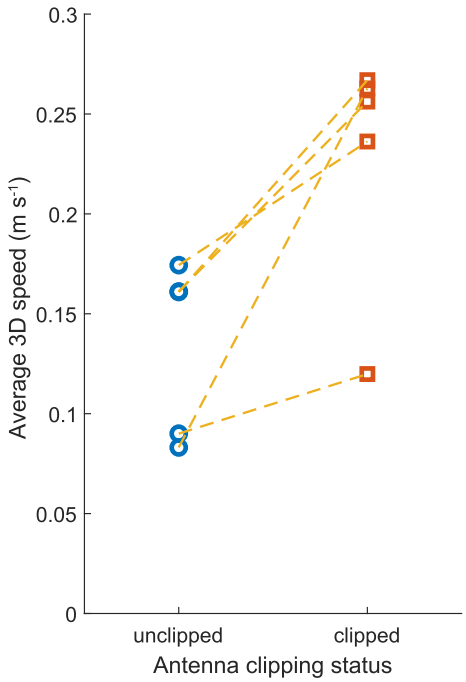

Fig. 6 Comparison of the average three-dimensional speed of five moths engaged in hovering flight pre- and post-antennectomy. Post-antennectomy moths had significantly faster speeds ($P = 0.0198$, paired t-test) signifying their more erratic in-flight positioning.

universal in the recovered moths and there were few consistent differences between flight posture or pitch dynamics pre- and post-antennectomy. Despite this, on the whole flight of post-antennectomy moths appeared more erratic and less consistent than that of intact animals. The clearest quantification of this effect came from comparing the average three-dimensional velocity measured at the abdomen–thorax junction during hovering flight in the recording chamber pre- and post-antennectomy (Fig. 6). This quantity was significantly larger post-antennectomy ($P = 0.0198$, paired t-test).

Summary

Here, we first reviewed some classic analyses of insect flight stability based on flapping-cycle averaged forces and torques, and then noted some plausible mechanisms that real animals might use to control their pitch orientation in response to endogenous or exogenous perturbations in the cycle-average framework. We next examined work on flight stability effects of the interaction of within-cycle variation in aerodynamic forces, torques, and body position. Finally, we provide some preliminary experimental data relevant for comparison to predictions from analytical and numerical models.

We find that our experimental pitch perturbation results are not a good match for a numerical simulation of flapping wing flight based on a blade-element model of flapping flight with aerodynamic coefficients from dynamically scaled (Usherwood and Ellington 2002) and computational fluid dynamics simulations (Zheng et al. 2013). Over the first complete flapping cycle following perturbation, the real moths slowed an externally imposed pitch velocity approximately three-fold faster than the blade-element model. This rapid response to perturbation is thus not consistent with basic flapping wing aerodynamics, including FCT. However, it is also not consistent with vibrational stabilization effects, which act over longer timescales. While it is possible that revisions to flapping wing force coefficients could bring the experiment and simulation back into alignment, these forces themselves are rooted in airfoil circulation, vortex development, and shedding, and are not necessarily as fast acting as is suggested by the experiment. We also believe that a neurosensory explanation for the discrepancy is unlikely because substantial deviations in flapping pattern were not seen, and even insects with synchronous flight muscle architectures like these hawkmoths may not be able to arbitrarily change their flapping pattern within a half flapping cycle. One possible mechanism bridging the gap between prediction and experimental result is fluid added mass. Because fluid added-mass effects act in response to acceleration, the extremely abrupt pitch acceleration provided by the projectile-based pitch perturbations may lead to unexpectedly large added-mass effects that are not included in the blade-element model, which primarily considers velocity-based fluid forces. Furthermore, theoretical work on added mass in animal locomotion and airfoils shows that in situations where there is asymmetry in shape fluid added mass can provide a virtual spring-like addition to the linearized flight mechanics (Kanso et al. 2005; Yan et al. 2014), providing a restoring torque bringing the animal back toward its original pitch orientation. We intended to further probe this possibility with further experiments and computational simulations in the near future.

Our experiments showing that moths recover flight capability approximately 24 h after antenna removal can be interpreted in a variety of ways. This does show that the antennal mechanosensory information is not necessary for stable flight in these animals. However, beyond that obvious finding, a variety of interpretations are possible. Flight capability could be regained by the nervous system adapting to ignore erroneous information from the antennal mechanosensors while prioritizing information from the visual system, sensing of wing deformation (Dickerson et al. 2014), or other intact sensory inputs. Alternatively, it is also consistent

with our finding that vibrational stability contributions to hovering flight render it stable, and neurosensory responses serve mainly to enhance this existing stability and increase the effectiveness and precision of flight maneuvers.

More broadly, the theoretical and experimental work presented here suggests that flight stability may be less of a challenge for large insects than is suggested by stroke-averaged and linearized flight dynamics models. However, miniaturization of insect body plans further challenges flight stability, and successful miniaturization of a flying insect body plan may also require enhancements to the neurosensory system and flight control responses.

Author contributions

T.H. and E.B. conceived the experiments. E.B. conducted the experiments. E.B. and T.H. analyzed the results. T.H., H.T., and E.B. wrote and reviewed the manuscript.

Acknowledgments

The authors thank Lillian Hewitt for assistance with video data analysis, and helpful comments from three referees.

Funding

This work was supported in part by funds from the National Science Foundation [IOS # 1253276 and CMMI # 2344214].

Conflict of interest

No conflict of interest is declared.

Data Availability statement

The underlying data for the results presented here are available in the FigShare repository at the following DOI: 10.6084/m9.figshare.25374661

References

Cheng B, Deng X. 2011. Translational and rotational damping of flapping flight and its dynamics and stability at hovering. IEEE Trans Robot 27:849–64.

Dahake A, Stöckl AL, Foster JJ, Sane SP, Kelber A. 2018. The roles of vision and antennal mechanoreception in hawkmoth flight control. eLife 7:e37606.

Dickerson BH, Aldworth ZN, Daniel TL. 2014. Control of moth flight posture is mediated by wing mechanosensory feedback. J Exp Biol 217:2301–8.

Dickinson MH, Lehmann FO, Sane SP. 1999. Wing rotation and the aerodynamic basis of insect flight. Science 284:1954–60.

Dickson WB, Polidoro P, Tanner MM, Dickinson MH. 2010. A linear systems analysis of the yaw dynamics of a dynamically scaled insect model. J Exp Biol 213:3047–61.

Dyhr JP, Morgansen KA, Daniel TL, Cowan NJ. 2013. Flexible strategies for flight control: an active role for the abdomen. J Exp Biol 216:1523–36.

Ellington CP, Van Den Berg C, Willmott AP, Thomas AL. 1996. Leading-edge vortices in insect flight. Nature 384:626–30.

Greeter JSM, Hedrick TL. 2016. Direct lateral maneuvers in hawkmoths. Biology open 5:72–82.

Greeter JSM. 2017. Damping at every turn: maneuvers and stability in the free flight of hawkmoth *Manduca sexta*. PhD thesis. Chapel Hill (NC): University of North Carolina at Chapel Hill.

Hedrick TL, Cheng B, Deng X. 2009. Wingbeat time and the scaling of passive rotational damping in flapping flight. Science 324:252–5.

Hedrick TL. 2008. Software techniques for two- and three-dimensional kinematic measurements of biological and biomimetic systems. Bioinspir Biomim 3:034001.

Kanso E, Marsden JE, Rowley CW, Melli-Huber JB. 2005. Locomotion of articulated bodies in a perfect fluid. J Nonlinear Sci 15:255–89.

Ristroph L, Ristroph G, Morozova S, Bergou AJ, Chang S, Guckenheimer J, Wang ZJ, Cohen I. 2013. Active and passive stabilization of body pitch in insect flight. J Roy Soc Interface 10:20130237.

Sane SP, Dieudonné A, Willis MA, Daniel TL. 2007. Antennal mechanosensors mediate flight control in moths. Science 315:863–6.

Sefati S, Neveln ID, Roth E, Mitchell TR, Snyder JB, MacIver MA, Fortune ES, Cowan NJ. 2013. Mutually opposing forces during locomotion can eliminate the tradeoff between maneuverability and stability. Proc Natl Acad Sci USA 110:18798–803.

Stengel RF. 2005. Flight dynamics. Princeton (NJ): Princeton University Press.

Sun M, Wang J, Xiong Y. 2007. Dynamic flight stability of hovering insects. Acta Mech Sinica 23:231–46.

Taha HE, Kiani M, Hedrick TL, Greeter JS. 2020. Vibrational control: a hidden stabilization mechanism in insect flight. Sci Robotics 5:eabb1502.

Taylor GK, Krapp HG. 2007. Sensory systems and flight stability: what do insects measure and why? Adv Insect Physiol, 34:231–316.

Taylor GK, Thomas AL. 2003. Dynamic flight stability in the desert locust *Schistocerca gregaria*. J Exp Biol 206:2803–29.

Theriault DH, Fuller NW, Jackson BE, Bluhm E, Evangelista D, Wu Z, Betke M, Hedrick TL. 2014. A protocol and calibration method for accurate multi-camera field videography. J Exp Biol 217:1843–8.

Usherwood JR, Ellington CP. 2002. The aerodynamics of revolving wings i. model hawkmoth wings. J Exp Biol 205:1547–64.

Yan Z, Taha HE, Hajj MR. 2014. Geometrically-exact unsteady model for airfoils undergoing large amplitude maneuvers. Aerosp Sci Technol 39:293–306.

Zhang C, Hedrick TL, Mittal R. 2019. An integrated study of the aeromechanics of hovering flight in perturbed flows. AIAA J 57:3753–64.

Zheng L, Hedrick TL, Mittal R. 2013. A multi-fidelity modelling approach for evaluation and optimization of wing stroke aerodynamics in flapping flight. J Fluid Mech 721:118–54.